Cell Transplantation
2017, Vol. 26(8) 1365-1379

DOI: 10.1177/0963689717720282
journals.sagepub.com/home/cll
SAGE

Engineered Microvasculature in PDMS Networks Using Endothelial Cells Derived from Human Induced Pluripotent Stem Cells

Amogh Sivarapatna[1], Mahboobe Ghaedi[2], Yang Xiao[1], Edward Han[1], Binod Aryal[3], Jing Zhou[1], Carlos Fernandez-Hernando[3], Yibing Qyang[4], Karen K. Hirschi[4], and Laura E. Niklason[1,2]

Abstract

In this study, we used a polydimethylsiloxane (PDMS)-based platform for the generation of intact, perfusion-competent microvascular networks in vitro. COMSOL Multiphysics, a finite-element analysis and simulation software package, was used to obtain simulated velocity, pressure, and shear stress profiles. Transgene-free human induced pluripotent stem cells (hiPSCs) were differentiated into partially arterialized endothelial cells (hiPSC-ECs) in 5 d under completely chemically defined conditions, using the small molecule glycogen synthase kinase 3β inhibitor CHIR99021 and were thoroughly characterized for functionality and arterial-like marker expression. These cells, along with primary human umbilical vein endothelial cells (HUVECs), were seeded in the PDMS system to generate microvascular networks that were subjected to shear stress. Engineered microvessels had patent lumens and expressed VE-cadherin along their periphery. Shear stress caused by flowing medium increased the secretion of nitric oxide and caused endothelial cells s to align and to redistribute actin filaments parallel to the direction of the laminar flow. Shear stress also caused significant increases in gene expression for arterial markers Notch1 and EphrinB2 as well as antithrombotic markers Kruppel-like factor 2 (KLF-2)/4. These changes in response to shear stress in the microvascular platform were observed in hiPSC-EC microvessels but not in microvessels that were derived from HUVECs, which indicated that hiPSC-ECs may be more plastic in modulating their phenotype under flow than are HUVECs. Taken together, we demonstrate the feasibly of generating intact, engineered microvessels in vitro, which replicate some of the key biological features of native microvessels.

Keywords

microvessels, microfluidics, human induced pluripotent stem cells (hiPSCs), endothelial cells, shear stress, arterial

Introduction

Vascular endothelial cells (ECs) line the entire circulatory system, including the large arteries as well as small capillary microvessels. Within different tissues, microvascular ECs possess unique functional and phenotypic features specific to that microenvironment.[1] However, current methods for EC culture in vitro rely on growing cells as 2-dimensional, flat monolayers, which does not recapitulate the complex microenvironmental context that is present in vivo. In addition, whereas the compressive modulus of endothelial basement membrane is in the range of 2 to 3 kpa,[2] the stiffness of tissue culture plastic is in the gigapascal range, which is far stiffer than most living tissues.[3] As such, primary ECs that

[1] Department of Biomedical Engineering, Yale University, New Haven, CT, USA
[2] Department of Anesthesiology, Yale University, New Haven, CT, USA
[3] Section of Comparative Medicine, Yale School of Medicine, Yale University, New Haven, CT, USA
[4] Department of Medicine, Section of Cardiovascular Medicine, Yale University, New Haven, CT, USA

Submitted: August 25, 2016. Revised: January 31, 2017. Accepted: February 15, 2017.

Corresponding Author:
Laura E. Niklason, Departments of Anesthesia and Biomedical Engineering, Yale University, 10 Amistad Street, Room 301D, New Haven, CT 06520, USA.
Email: laura.niklason@yale.edu

are cultured on tissue culture plastic rapidly dedifferentiate, downregulating important genes and losing their specialized characteristics.[4] Furthermore, in vitro culture raises the basal turnover rate of ECs to 1% to 10% per day, from roughly 0.1% per day in vivo.[5]

To date, significant headway has been made in microsystems engineering, and multiple groups have described biomimetic microfluidic cell culture systems. These systems are populated with living human cells, have micrometer (5 to 200 μm) scale resolution with physiologically relevant microarchitectural details, and can be continuously perfused, overcoming many of the constraints of statically cultured monolayers of cells.[6-9] In particular, polydimethylsiloxane (PDMS), a polymeric organosilicon material, has many benefits: It is transparent, gas permeable, deformable and exhibits low autofluorescence. Detailed protocols now exist for the development of reproducible microfluidic platforms that can apply defined biochemical and mechanical stimuli to multiple cell types interacting over distances of less than 1 mm.[10-12] Although several tools are available for the study of microvessel function in vitro, there still exist significant knowledge gaps with regard to some of their key biological features, such as nitric oxide (NO) production, antithrombotic, and anti-inflammatory phenotype, as well as arterial versus venous specification in response to flow.

Human induced pluripotent stem cells (hiPSCs) represent a powerful platform for studying vascular biology for several reasons, including the ability to generate tissue-specific cells, including EC subtypes such as microvascular ECs,[13] and the ability to scale up to derive an unlimited quantity of cells for tissue engineering applications. We previously reported the generation of large numbers of functional ECs derived from hiPSCs using an embryoid body (EB)-based differentiation protocol. We found that these cells could be matured into an arterial-like phenotype under shear stress in a biomimetic, large vessel flow bioreactor.[14] We also demonstrated the plasticity[15] of hiPSC-ECs, which have never been exposed to flow, as compared to primary human ECs, in taking on a more vasoprotective phenotype.[16] Thus, it appears that hiPSC-ECs respond to biomechanical cues and can be directed toward specific EC subtypes.

Recent work has shown that temporal activation of Wnt signaling through the small molecule glycogen synthase kinase 3β (GSK3β) inhibitor CHIR99021 (referred to here as CHIR) can drive large numbers of hiPSCs toward an EC or endothelial progenitor cell-like state in the absence of growth factors.[17,18] The likely mechanism of endothelial specification and induction by CHIR is through the Wnt/β-catenin signaling pathway, in which β-catenin accumulates and travels to the nucleus to activate Wnt to target gene expression.[18] This protocol for the quick induction of EC progenitors from hiPSCs bypasses many of the limitations of previously published methods by significantly reducing differentiation time, avoiding fragile EB formation steps, and eliminating serum and growth factors from the differentiation medium completely.

In this study, we sought to establish a microvascular platform for generating, in vitro, functional microvessals derived from ECs that were differentiated from transgene-free hiPSCs under chemically defined, growth factor-free conditions. We developed a PDMS-based platform for the generation of intact, perfusable hiPSC-EC microvessel networks in vitro. Shear stress caused by flowing medium increased the secretion of NO, caused ECs to align and redistribute actin filaments parallel to the direction of the laminar flow, and also caused significant increases in gene expression for arterial markers Notch1 and EphrinB2, as well as antithrombotic markers Kruppel-like factor 2 (KLF-2)/KLF-4. These changes in response to shear stress in the microvascular platform were observed in hiPSC-ECs but not in microvessels that were derived from human umbilical vein endothelial cells (HUVECs), which indicated that hiPSC-ECs are more plastic in modulating their phenotype under flow than are HUVECs.

Materials and Methods

Cell Culture

Human iPSCs (hiPSCs) were maintained on Matrigel as previously described.[19,20] Briefly, hiPSCs were propagated on human embryonic stem cell (hESC)-qualified Matrigel (BD Biosciences, San Jose, CA, USA) from passages 25 to 40 and maintained in mTeSR medium (Stemcell Technologies, Vancouver, Canada). Medium was replaced daily, and hiPSC colonies were routinely passaged every 5 to 7 d by mechanical dissociation using dispase (Stemcell Technologies). All hiPSCs expressed typical pluripotency markers, including octamer-binding transcription factor 4 (Oct4), sex-determining region Y-box 2, and Nanog as assessed by immunostaining (data not shown). The hiPSC line Y6, utilized here, was generated from healthy female neonatal fibroblasts using the genome integration-free Sendai virus. The episomal hiPSC line was purchased from WiCell (Madison, WI, USA). Both cell types were used for experiments with emphasis on the Y6 cells since they provided optimal EC differentiation.

Primary human ECs, including pooled primary HUVECs, were obtained from the Yale University Vascular Biology and Therapeutics Tissue Culture Core Facility. Human aortic endothelial cells (HAECs) were purchased from PromoCell (Heidelberg, Germany). Both cell types were maintained in VascuLife vascular endothelial growth factor (VEGF) medium (Lifeline Cell Technology, Frederick, MD, USA). All cells were routinely passaged at 80% confluence every 3 to 4 d and used between passages 2 to 5 (P2 to P5). Both HUVECs and HAECs were used in experiments as rigorous controls for differentiated venous and arterial cells, respectively.

2D in vitro Differentiation and Isolation of hiPSC-ECs

hiPSCs were differentiated into ECs using an adapted 2D, serum and growth factor-free protocol.[18] Briefly, when

hiPSC colonies reached approximately 80% confluence (day 1), the mTeSR medium was aspirated, and the wells were washed once with 1× phosphate-buffered saline (PBS). Then, differentiation medium consisting of advanced Dulbecco's modified eagle medium (DMEM)/F12 supplemented with 2.5 mM GlutaMAX, and 60 μg/mL ascorbic acid (Sigma-Aldrich, A8960, St, Louis, MO, USA) as well as 10 μM CHIR99021 was added. Fresh medium (2 mL per well of 6 well plate) containing 10 μM CHIR99021 was added the next day. On day 3, medium was replaced with the basal medium containing no CHIR99021. On day 5, cells were harvested for isolation.

For isolation of ECs from differentiated colonies, wells were washed with PBS, and accutase was added for 7 min at 37 °C. Cells were pipetted vigorously to ensure single-cell suspension and were filtered through a 40 μm nylon mesh and centrifuged at 1,000 rpm for 5 min. Then, a CD31 magnetic bead (Dynabeads, Invitrogen, Thermo Fisher Scientific, Carlsbad, CA, USA) isolation kit was used according to manufacturer's protocol. Briefly, approximately 2 million cells (per 6-well plate) were incubated with 20 μL of Dynabeads in PBS + 0.1% bovine serum albumin (BSA) for 20 min at 4 °C with rocking, followed by placing tube in magnet and washing to remove non-CD31+ cells. After isolation, CD31+ hiPSC-ECs (passage 0 [P0]) were plated on fibronectin-coated plates (3 μg/cm^2) in expansion medium–containing VascuLife VEGF medium + 5 ng/mL VEGF. Once confluent, cells were passaged routinely and plated at 10,000 cells/cm^2. Cells up to P5 were used for experiments.

PDMS Microfluidic System: Fabrication and Design

Microfluidic devices were made of PDMS (Silgard 184, Dow-Corning, Midland, MI, USA) through soft lithography techniques.[11] The microchannels of the PDMS chip had a height of 110 μm, and channel widths varying between 80 and 200 μm, with the overall device area being 4 mm × 8 mm. The mold for the PDMS replica was a negative photoresist SU-8 micropatterned silicon wafer. It was pretreated with trimethylchlorosilane (Sigma-Aldrich) vapor for 30 min to facilitate PDMS release. PDMS prepolymer elastomer base and curing agent were mixed completely (parts A and B in 10:1 ratio), poured onto the silicon master, and cured in the oven at 80 °C for 1 h. After curing, inlets and outlets were punched using a punch press (Schmidt Technology, Cranberry Twp, PA, USA), and the PDMS layer was bonded to glass slides (Superfrost Microscope Slides, Thermo Fisher Scientific, Waltham, MA) after 30 s of oxygen plasma treatment. After the devices were assembled, they were put in an 80 °C oven for an hour to strengthen the bonding.

Computational Modeling of Microvascular Network

COMSOL Multiphysics (Version 4.0.0.982, COMSOL Inc., Burlington, MA, USA) software was used to perform finite element analysis and model the flow conditions inside the microfluidic device (Fig. 1A and C). A stationary laminar flow model utilizing the Navier–Stokes and continuity equations on an incompressible fluid were used. A 3D model of the device was constructed in COMSOL with a no-slip wall boundary condition. Cell culture media density of 1,020 kg/m^3 [6] and a viscosity of 0.8 cP[21] were used as a reference. A flow rate of 10 μL/min was used for the inlet boundary condition (corresponding to actual experimental flow rates applied to the device), while a pressure of 0 Pa was used for the outlet boundary condition.

Cell Seeding and Microvessel Formation

To improve hydrophilicity of the PDMS and to facilitate cell attachment, devices were filled with 5 μg/mL rat tail collagen type I (9.27 mg/mL, Corning Inc., Ref. 354249, Corning, NY, USA) and placed in a 37 °C incubator for at least 1 h. Devices were then perfused with cell culture medium to flush out excess collagen. For cell seeding, hiPSC-ECs or HUVECs at a concentration of 5 × 10^6 cells/mL were prepared, and approximately 100 μL of the cell suspension was loaded into the inlet of the microfluidic device, allowing the cells to flow through the device and seed uniformly via gravity-driven flow. The inlet and outlet ports were created from blunt tip needles (23G, Becton Dickinson, Ref. 427565, Franklin Lakes, NJ, USA). The devices were then placed in the incubator at 37 °C for 2 h to allow cells to attach. The medium was then replenished with fresh medium and placed back into the incubator. Devices were cultured for 4 to 7 d with medium replenishment (200 μL) occurring twice per day in nonflowing cultures.

Shear Stress Application

In order to simulate the physiological levels of flow that exist in vivo, shear stress was applied to microvessels. A syringe pump (Legato 100, KD Scientific, Holliston, MA, USA) was used at a flow rate of 10 μL/min, corresponding to roughly 0.1 to 11.3 dyne/cm^2 in wall shear stress in the device, based upon COMSOL simulations. Briefly, a 20 cc syringe, containing medium, was placed at the infusion site at the pump. The needle from the syringe was connected to flexible plastic tubing (Tygon, Saint-Gobain, Corp, AAQ04103, Malvern, PA, USA) with an inner diameter of 0.020 inches and an outer diameter 0.060 of inches. On the other end of the plastic tubing was an L-shaped hollow pin, which connected to the inlet on the microfluidic device. At the outlet of the microfluidic device was another hollow pin connected to plastic tubing, leading to a 15 mL conical tube, which acted as a reservoir to collect spent medium.

Vascular Tube Formation Assay and TNF-α Stimulation for ICAM Expression

To assess the angiogenic capacity of hiPSC-ECs in vitro, a thin layer of Matrigel (BD Biosciences) was used to coat the

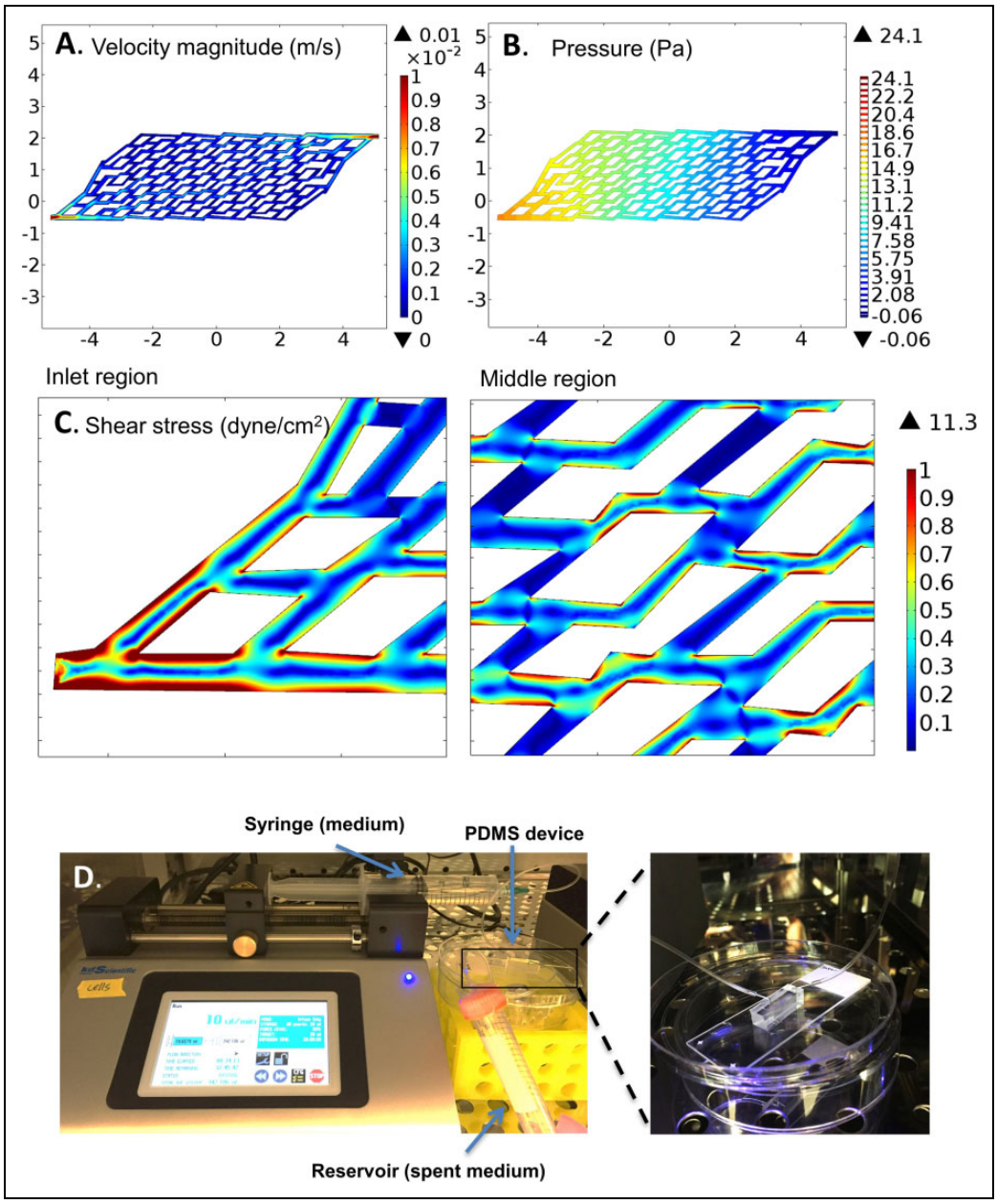

Fig. 1. In silico modeling of microvascular network using COMSOL shows (A) velocity magnitude (m/s) distribution profile in the device is symmetrical after encountering bifurcation points near the inlet and outlet. (B) Pressure (Pa) gradient exists in the device, decreasing uniformly from high to low (from inlet to outlet, respectively) after gravity-driven loading of medium. (C) Simulated wall shear stress (dyne/cm^2) profile, at a flow rate of 10 μL/min, at inlet of device (left) and middle of device (right). (D) Syringe pump setup showing syringe-containing medium (top) connecting to inlet of polydimethylsiloxane (PDMS) device (middle) with the outlet leading to a 15 cc conical tube reservoir (bottom) to collect spent medium. Right shows blown up image of fully connected PDMS device.

wells of a 48-well plate, followed by seeding with 5×10^4 cells directly in a minimal volume of medium. After 24 h, wells were fixed in 4% paraformaldehyde (PFA), and networks were imaged using a phase-contrast microscope.

To assess the functionality of hiPSC-ECs in response to cytokine stimulation, 10 ng/mL (final concentration) of tumor necrosis factor α (TNF-α) was added to hiPSC-ECs for 15 h. Cells were harvested and compared with HUVECs by Western blotting for induction of intracellular adhesion molecule 1 (ICAM-1 expression). Negative control cells were untreated with hiPSC-ECs and HUVECs.

Immunohistochemistry

For immunofluorescence analysis, cells were seeded into 4-well chamber slides and allowed to reach confluence. They were then washed with PBS and fixed in 4% PFA in PBS for 20 min at room temperature (RT). Cells were then

Table 1. Sequences of Primers Used in Quantitative Real-time Polymerase Chain Reaction.

Gene	Length (bp)	Forward Primer	Reverse Primer
CD31	134	TGCAGTGGTTATCATCGGAGTG	CGTTGTTGGAGTTCAGAAGTG
CD144	80	TCACCTGGTCGCCAATCC	AGGCCACATCTTGGGTTCCT
KDR	90	TGCCTCAGAAGAGCTGAAAAC	CACAGACTCCCTGCTTTTGCT
EphrinB2	107	GTTCCGGCGTTTATTTCTG	CCACAGCTAAATCGTCACC
Notch1	132	CACGCGGATTAATTTGCATC	TCTTGGCATACACACTCCG
Connexin40	198	CTGCTAGGGAGTCACTGTACAC	CTGGTCAGGGTTCGAGAGAG
CXCR4	102	CACCGCATCTGGAGAACCA	GCCCATTTCCTCGGTGTAGTT
COUPTFII	77	GCCATAGTCCTGTTCACCTC	CTGAGACTTTTCCTGCAAGC
EphB4	164	TGAAGAGGTGATTGGTGCAG	AGGCCTCGCTCAGAAACTCAC
KLF2	102	ACTTTCGCCAGCCCGTGC	AGTCCAGCACGCTGTTGAG
KLF4	93	CGAACCCACACAGGTGAGAA	TACGGTAGTGCCTGGTCAGTTC
Jag2	61	GATACCACCCCGAATGAGGAG	GGGTTGATCATGCCGGC
Tie 2	135	GCTAGAGTCAACACCAAGGC	TCCAAGAAATCACAGCTGAGG
eNOS	79	GGAACCTGTGTGACCCTCA	CGAGGTGGTCCGGGTATCC
Ang-1	120	CCTACACTTTCATTCTTCCAG	TCTGGGAAGAGAAATCCGGT
Prox-1	119	CCCAGGACAGTTTATTGACCGA	GGTTGTAAGGAGTTTGGCCCAT
T1α	185	AGAGCAACAACTCAACGGGAA	TTCTGCCAGGACCCAGAGC
CXCR4	79	CACCGCATCTGGAGAACCA	GCCCATTTCCTCGGTGTAGTT
ZO-1	63	TGATCATTCCAGGCACTCG	CTCTTCATCTCTACTCCGGAGACT
GAPDH	122	GACAACAGCCTCAAGATCATCAG	ATGGCATGGACTGTGGTCATGAG

permeabilized and blocked for nonspecific antigen binding with PBS + 10% fetal bovine serum (FBS) + 0.1% Triton X-100 for 1 hour at RT. The cells were then incubated with primary antibodies against platelet and endothelial cell adhesion molecule 1 (CD31; Abcam, ab28364, Cambridge, UK), vascular endothelial (VE)-cadherin (CD144; Santa Cruz Biotechnology, sc-6458, Dallas, TX, USA), endothelial nitric oxide synthase (eNOS; Abcam, ab5589), von Willebrand factor (vWF; Abcam, ab6994) overnight at 4 °C. The next day, cells were washed 3 times with 1× PBS and incubated with corresponding secondary antibody (1:500) for 2 h at RT. After washing 3 times with 1× PBS, mounting medium–containing 4,6-diamidino-2-phenylindole (DAPI) (Vector Laboratories, Burlingame, CA, USA) was applied to slides to visualize nuclei, and coverslips were placed to seal slides. The slides were visualized using a Leica camera (Wetzlar, Germany) DMI6000 B fluorescence microscope. Confocal microscopy was used to visualize luminal structures in microvessel PDMS devices by taking *z*-stacks of the entire width of the device (200 μm) with slice widths of approximately 5 μm.

Real-Time Polymerase Chain Reaction (RT-PCR)

Quantitative RT-PCR was used to determine the expression of endothelial markers in differentiated cells from hiPSCs, cultured in the bioreactor and in static conditions. Cells from the microfluidic device were harvested by adding accutase (Innovative Cell Technologies, San Diego, CA, USA) through the inlet for 5 min to allow cells to detach and were extracted from the outlet using a blunt tip needle, followed by immediately washing of the cells and freezing the cell pellet. Adult human primary HUVECs and HAECs were used as controls. Briefly, total cellular RNA was prepared using the RNeasy Mini Kit (Qiagen, Hilden, Germany) following the manufacturer's instructions. Single-stranded cDNA was synthesized using the reverse transcription-PCR protocol of the first-strand cDNA synthesis kit from Invitrogen (Thermo Fisher Scientific). Quantitative real-time PCR was performed using SYBR Green PCR Supermix (Bio-Rad Laboratories, Hercules, CA, USA). Concentrations of all primers were optimized before use. PCR conditions included an initial denaturation step of 4 min at 95 °C, followed by 40 cycles of PCR consisting of 15 s at 95 °C, 30 s at 60 °C, and 30 s at 72 °C. Each sample was run in triplicate. The comparative Ct value method using glyceraldehyde 3-phosphate dehydrogenase (GAPDH) as a housekeeping gene for an internal standard was employed to determine the relative levels of gene expression. Ct values from the triplicate PCR reactions for a gene of interest (GOI) were normalized against average GAPDH Ct values from the same complementary DNA sample. Fold change of GOI transcript levels between sample A and sample B $= 2^{-\Delta\Delta Ct}$, where $\Delta Ct =$ Ct(GOI) – Ct(GAPDH) and $\Delta\Delta Ct = \Delta Ct(A) - \Delta Ct(B)$. Primers that were used in this study are listed in Table 1.

Western Blotting

Approximately 1 million cells were lysed, and 30 mg of protein was loaded on a 4% to 12% sodium dodecyl sulfate polyacrylamide electrophoresis gel (SDS-PAGE) (Bio-Rad Laboratories) for Western blot analysis. Anti-ICAM-1 antibody (R&D Systems BBA17, Minneapolis, MN, USA) 1:1,000, anti-CD31 (Abcam 28364) 1:400, anti-VE-cadherin 1:100 (Santa Cruz Biotechnology SC6458), anti-β-catenin 1:100 (eBioscience Inc. 14-2567, Santa Clara, CA, USA),

anti-Notch1-ICD 1:400 (Abcam 8925), anti-EphrinB2 1:1,000 (Abcam ab96264), anti-β-tubulin 1:4,000 (Genetex GTX628802, Irvine, CA, USA), and anti-HSP90 1:1,000 (BD Biosciences 610419) were used to probe for proteins of interest overnight at 4 °C. Blots were washed and incubated with 1:5,000 Alexa Flour 680 rabbit anti-goat, goat anti-mouse, or donkey anti-rabbit secondary antibodies for 1 h. Protein bands were visualized using the Odyssey Infrared Imaging System (LI-COR Biosciences, Lincoln, NE, USA. Densitometry analysis of the gels was carried out using ImageJ software from the National Institutes of Health (NIH, Bethesda, MD, USA; http://rsbweb.nih.gov/ij/).

Statistical Analyses

All experiments were repeated at least 3 times, and each condition was analyzed in triplicate. Data are presented as the means ± standard error of the mean (SEM) for quantitative variables. An unpaired Student's *t*-test was performed to evaluate whether the 2 groups were significantly different from each other. A P value of ≤ 0.05 (2-tailed) was considered statistically significant, except in Fig. 2, where a P value of ≤ 0.02 (2-tailed) was considered statistically significant. All statistical analysis was performed in Microsoft Excel (Microsoft, Redmond, WA, USA).

Results

Evaluation of EC Marker Expression in Differentiating hiPSC-ECs

hiPSCs were differentiated into ECs using an adapted 2D, serum, and growth factor-free protocol (Fig. 3A).[18] The endothelial marker CD31 was significantly higher on day 5 as compared to day 1 of differentiation by qRT-PCR. VE-cadherin was significantly higher on days 4 and 5, while kinase insert domain receptor (KDR) was significantly higher on day 5, as assessed by qRT-PCT (Fig. 3B to D). This method relied on rapidly inducing mesoderm cells in the first 2 d (Fig. 3E) using CHIR, then switching cells to a simple basal medium consisting of Advanced DMEM/F12 supplemented with 2.5 mM GlutaMAX, and 60 µg/mL ascorbic acid (Sigma-Aldrich, A8960) from day 3 to day 5 to obtain EC progenitors (Fig. 3F), followed by isolation of hiPSC-ECs (Fig. 3G).

On day 5, immunofluorescence analysis of differentiating cells revealed robust expression of VE-cadherin+ cells (Fig. 3H to J). Western blot analysis demonstrated that both VE-cadherin (Fig. 3 K) and CD31 (Fig. 3 L) expression was present in day 5 differentiating cells while not in hiPSCs.

Effect of CHIR on Vascular and Arterial-Like Marker Expression in Differentiating hiPSC-ECs

Connexin 40 is widely distributed in the endothelium of large arteries,[22] while protein jagged-2 (Jag2) is a Notch ligand expressed by arterial ECs in mice;[23] and tyrosine kinase with immunoglobulin and epidermal growth factor homology domains (Tie2) is involved in vascular stabilization and remodeling. We found that Connexin 40 and Jag2 gene expression were significantly higher on day 5 as compared to day 1, whereas Tie2 gene expression did not significantly change (Fig. 2A and C, $P < 0.02$ compared to day 1 of differentiation). These data are consistent with a potential for arterial-like phenotype in early differentiating ECs using this hiPSC differentiation strategy.

In order to confirm this, we next looked at an important signaling pathway in inducing an arterial phenotype, the Notch pathway. *Notch1* gene expression was found to be significantly upregulated on day 5 of differentiation as compared to day 1 (Fig. 2D). Also, Western blot analysis showed appreciable Notch1-actived (NICD) protein on days 1 to 5. NICD was also expressed in HUVEC controls and at a very low level in HAECs, which could be due to multiple passages in culture (Fig. 2E). We next looked at the expression of EphrinB2, an arterial marker that is downstream of the Notch pathway. Although EphrinB2 messenger RNA (mRNA) expression was significantly higher on day 5 as compared to day 1, strong protein expression was detectible on days 1 to 5 (Fig. 2F and G). In fact, quantitative densitometry showed significantly higher levels of expression as compared to arterial control cells, HAECs, on days 4 and 5, whereas there were almost undetectable levels in day 0 hiPSCs (Fig. 3G, bottom graph). Taken together, these data show that the differentiation protocol was inducing activation of the Notch1 pathway in differentiating hiPSCs, and activation of EphrinB2 expression. This induction is visible at both the mRNA and protein levels, and is comparable to, or higher than, what is observed in culture-expanded human arterial endothelium.

Characterization of Isolated hiPSC-ECs

Isolated hiPSC-EC populations were expanded and assessed after CD31 magnetic bead isolation on day 5 of differentiation. Initial isolated hiPSC-ECs were allowed to grow to confluence and termed passage 0 (P0) cells, and subsequent characterization occurred between P1 and P3. Immunohistochemistry revealed robust expression of CD31, VE-cadherin, vWF, eNOS, and some Ephrin type-B receptor 4 (EphB4) positivity (Fig. 4A to E). hiPSC-ECs form networks when cultured on Matrigel (Fig. 4F). Gene expression analysis using qRT-PCR demonstrated hiPSC-ECs have significantly higher levels of the general EC marker KDR, arterial markers Notch 1, EphrinB2, and Connexin 40, and significantly lower levels of venous marker chicken ovalbumin upstream promoter transcription factor 2 (COUP-TFII) and lymphatic marker prospero homeobox protein 1 (Prox-1) when compared to HUVEC controls ($P < 0.05$; Fig. 4G and H). They also have comparable levels of CD31 and VE-cadherin compared to HUVECs (Fig. 4G). Similarly, Western blots demonstrated comparable protein level expression of CD31 compared to HUVEC (Fig. 4I). Expression of ICAM-1 (100 kD band) in hiPSC-ECs was induced after treatment with TNF for 15 h (Fig. 4 J, tubulin-loading

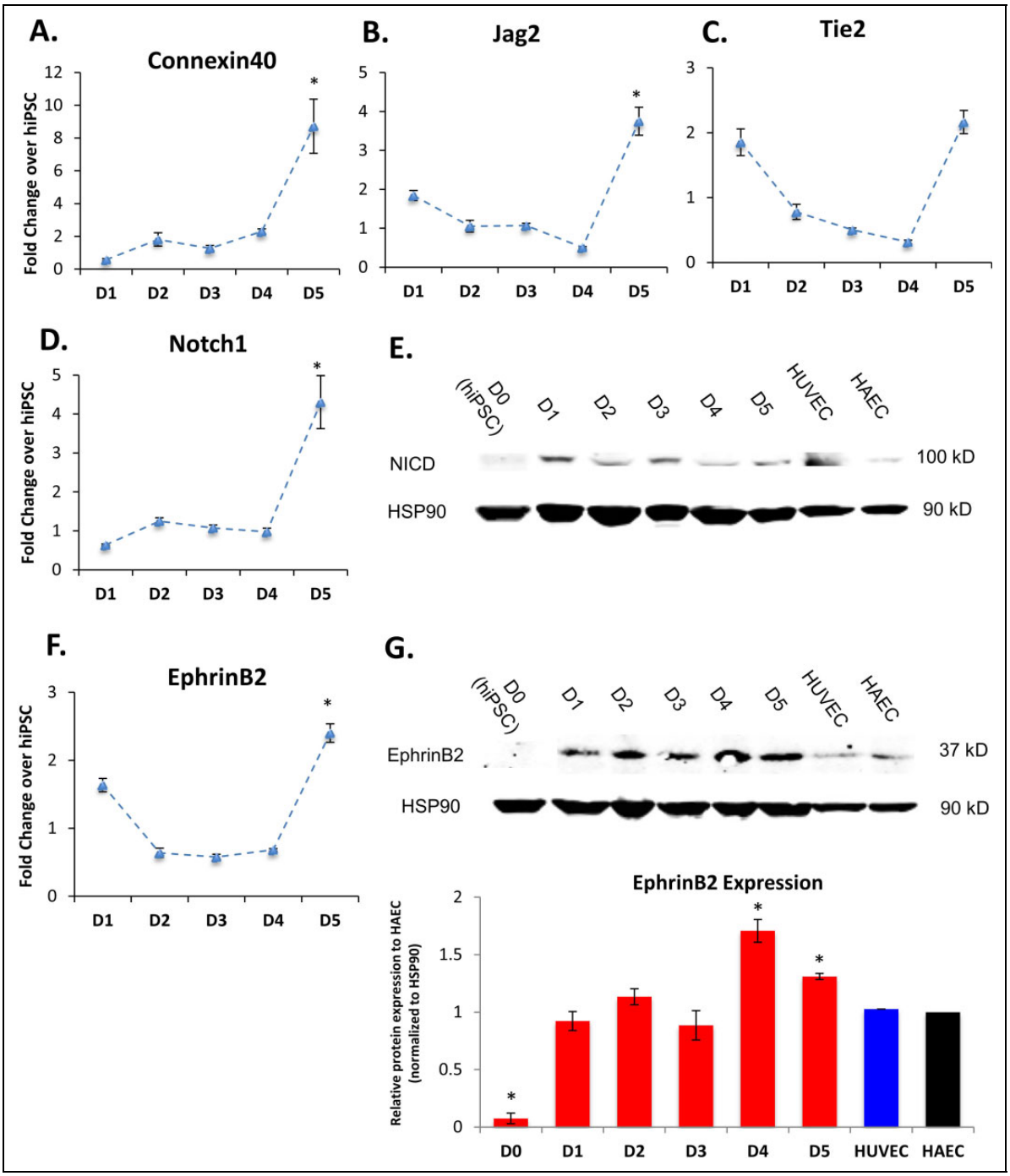

Fig. 2. Quantitative real-time reverse transcription polymerase chain reaction **(**qRT-PCR) showing the time course for the upregulation of arterial endothelial cell (EC)-specific genes (A) Connexin 40, (B) protein jagged-2 (Jag2), and (C) tyrosine kinase with immunoglobulin and epidermal growth factor homology domains (Tie2) over 5 d (D1–D5). (D) qRT-PCR showing the time course for upregulation of Notch1, and (E) Western blot demonstrating the protein-level expression of Notch1-activated (NICD, 100 kD band) from day 0 (D0) of differentiation all the way through day (D5) compared to human umbilical vein endothelial cell (HUVEC) and human aortic endothelial cells HAEC controls (left to right, heat shock protein 90 [HSP90] used as loading control, bottom). (F) qRT-PCR showing the time course for upregulation of the arterial marker EphrinB2 from day 0 to day 5 (D1-D5). Asterisks in A-F indicate $P < 0.02$ compared to day 1 of differentiation. (G) Western blot demonstrating the protein-level expression of EphrinB2 (37 kD band) from day 0 (D5) of differentiation all the way through day 5 (D5) compared to HUVEC and HAEC controls. Bottom graph shows quantitative densitometry of EphrinB2 expression relative to HAECs over 5 d, with asterisks indicating $P < 0.05$ compared to HAECs, demonstrating a significant increase on days 4 and 5. For qRT-PCR, values from 3 independent experiments from the triplicate polymerase chain reaction (PCR) reactions for genes of interest were normalized against average glyceraldehyde 3-phosphate dehydrogenase (GAPDH) Ct values from the same complementary DNA (cDNA) sample. Fold change of gene of interest (GOI) transcript levels between samples equals $2\text{-}\Delta\Delta Ct$, where $\Delta Ct = Ct(GOI) - Ct(GAPDH)$, and $\Delta\Delta Ct = \Delta Ct(ATII) - \Delta Ct(ATII)$. For all panels, data represent at least 3 observations for each experiment and are expressed as mean values $\pm$ standard error of mean [SEM].

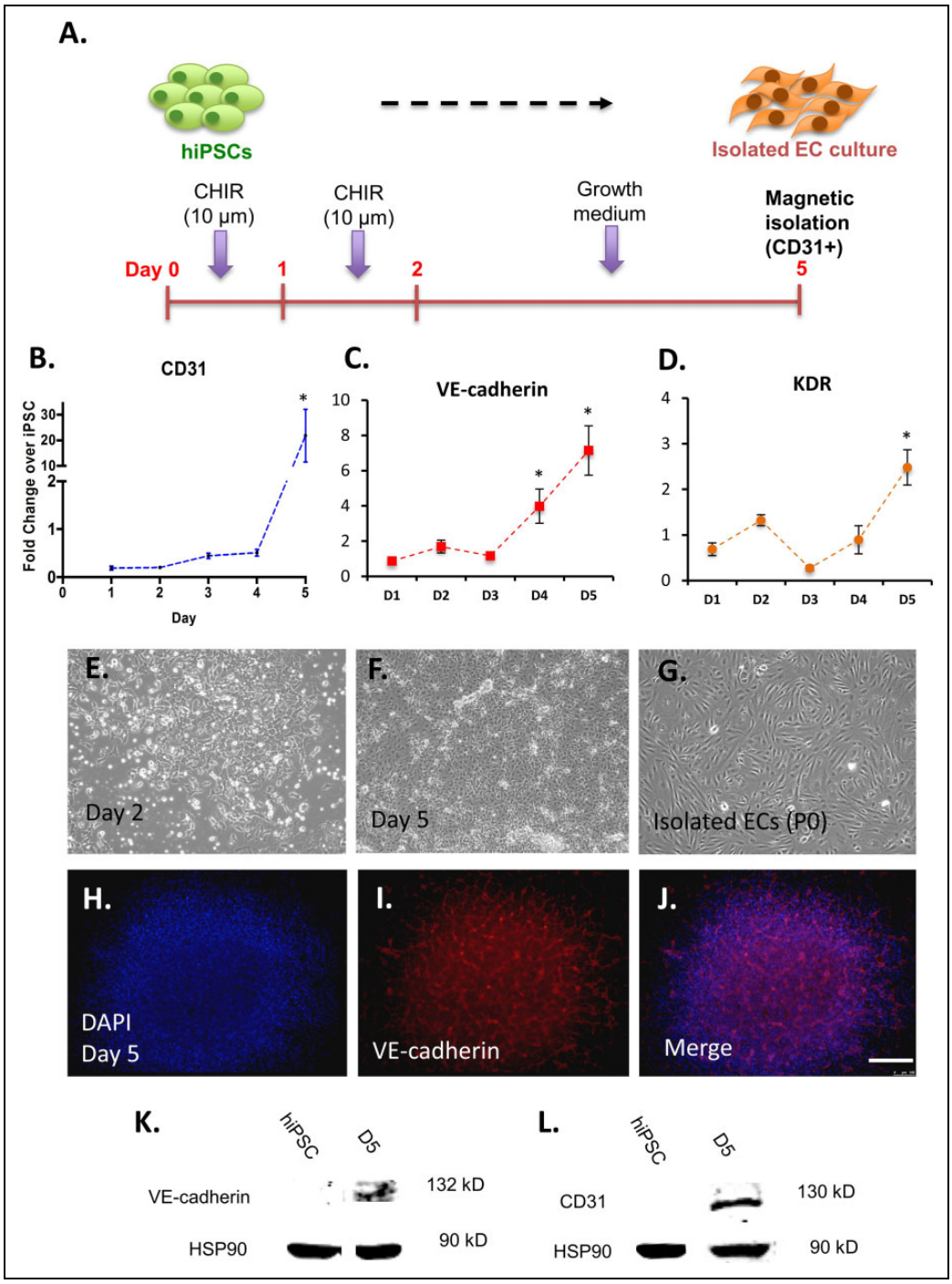

Fig. 3. (A) Schematic for directed differentiation protocol of human induced pluripotent stem cell-derived endothelial cells (hiPSC-ECs) in vitro in 5 d via a 2D monolayer approach using the small molecule glycogen synthase kinase 3β inhibitor CHIR99021. Quantitative real-time reverse transcription polymerase chain reaction (qRT-PCR) showing the time course for the upregulation of the endothelial cell (EC)-specific genes (B) CD3, (C) vascular endothelial (VE)-cadherin, and (D) kinase insert domain receptor (KDR) over 5 d (D1-D5). Asterisks indicate $P < 0.05$ compared to D1. Phase contrast images of (E) early mesodermal cells at day 2 (F) endothelial or endothelial-progenitor cells at day 5 and (G) isolated P0 hiPSC-ECs (via CD31+ magnetic bead selection) at confluence, showing typical EC cobblestone morphology. Immunofluorescence staining of typical differentiating hiPSC colony at day 5 showing (H) nuclei via 4',6-diamidino-2-phenylindole (DAPI, blue) (I) emerging VE-cadherin positive cells (red) and (J) merge of DAPI and VE-cadherin, scale bar = 200 µm. (K) Western blot showing no expression of VE-cadherin (132 kD band) in hiPSCs (left) and strong expression on day 5 of differentiation (D5, right) with HSP90 (bottom) used as loading controls. (L) Western blot showing no expression of CD31 (130 kD band) in hiPSCs (left), and strong expression on day 5 of differentiation (D5, right) with HSP90 (bottom) used as loading controls. For qRT-PCR, values from 3 independent experiments from the triplicate PCR reactions for genes of interest were normalized against average GAPDH Ct values from the same complementary DNA (cDNA) sample. Fold change of GOI transcript levels between samples equals $2\text{-}\Delta\Delta Ct$, where $\Delta Ct = Ct(GOI) - Ct(GAPDH)$, and $\Delta\Delta Ct = \Delta Ct(ATII) - \Delta Ct(ATII)$. (Error bar indicates ± standard error of mean [SEM] and n = 3 independent experiments).

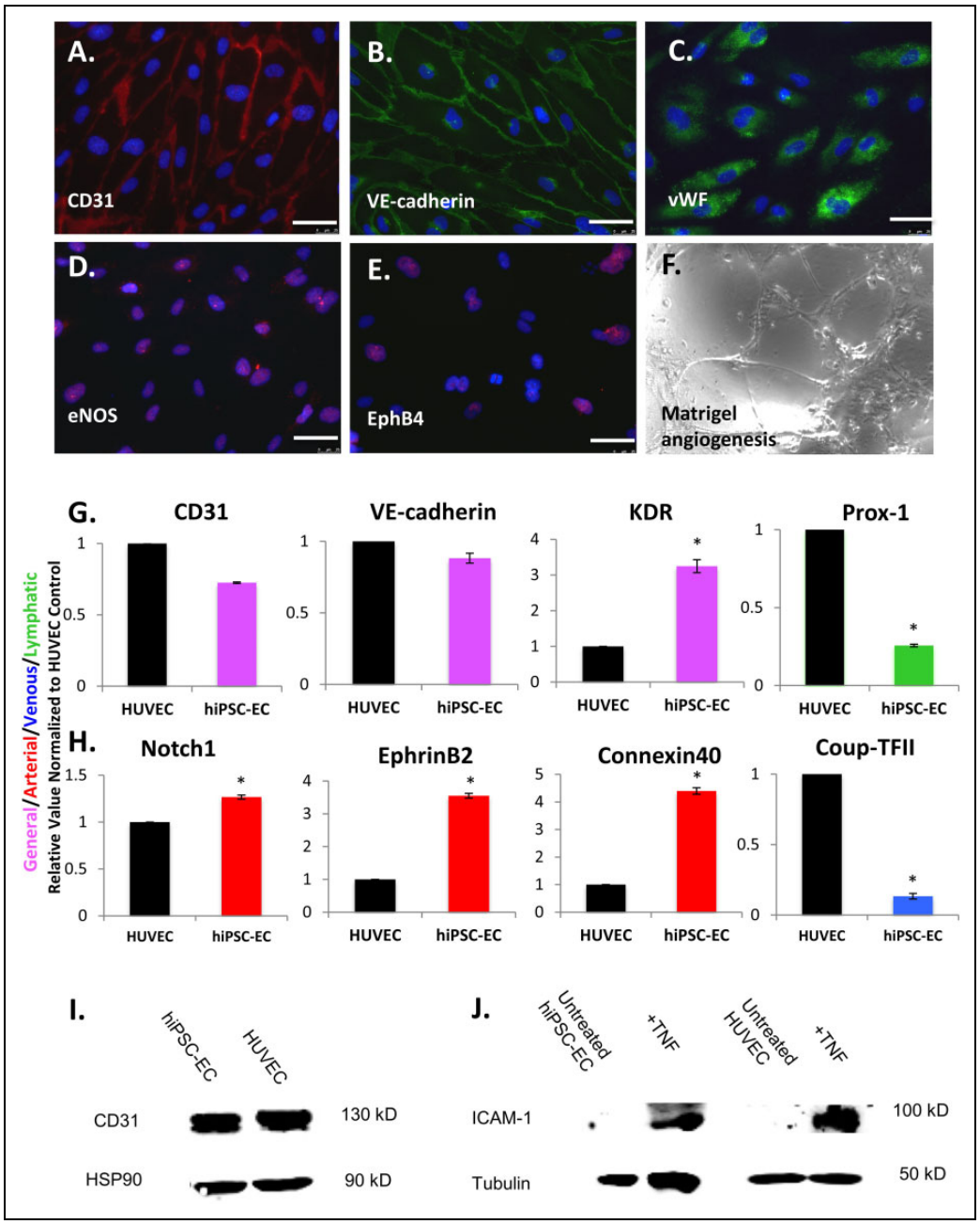

Fig. 4. Immunofluorescence analysis of selected endothelial cell (EC) markers in human induced pluripotent stem cell-derived endothelial cells (hiPSC-ECs) after differentiation, isolation, and expansion for 2 to 3 passages on fibronectin-coated plates shows expression of (A) CD31, (B) vascular endothelial (VE)-cadherin, (C) von Willebrand factor (vWF), (D) endothelial nitric oxide synthase (eNOS), and (E) Ephrin type-B receptor 4 (EphB4). A functional assay demonstrates that hiPSC-ECs (F) form networks when cultured on Matrigel-coated plates for 24 h. Scale bars = 25 μm. Quantitative real-time reverse transcription polymerase chain reaction (qRT-PCR) analysis of endothelial cells (EC) gene expression in hiPSC-ECs, relative to human umbilical vein endothelial cells (HUVECs), for (G) general EC markers CD31, vascular endothelial (VE)-cadherin and kinase insert domain receptor (KDR; pink), lymphatic marker prospero homeobox protein 1 (Prox-1; green), and (H) arterial markers Notch1, EphrinB2, and Connexin 40 (red) and venous marker chicken ovalbumin upstream promoter transcription factor 2 (Coup-TFII; blue), with asterisks indicating $P < 0.05$ compared to HUVECs. Western blot showing (I) strong CD31 expression (130 kD band) in isolated hiPSC-ECs compared to HUVECs with HSP90 loading control and (J) expression of intracellular adhesion molecule 1 (ICAM-1; 100 kD band) in hiPSC-ECs after treatment with tumor necrosis factor (left) and in HUVECs (right) with tubulin-loading controls, demonstrating comparable levels of induction. (Error bar indicates ± standard error of mean [SEM] and $n = 3$ independent experiments. Asterisks indicate $P < 0.05$ compared to HUVECs).

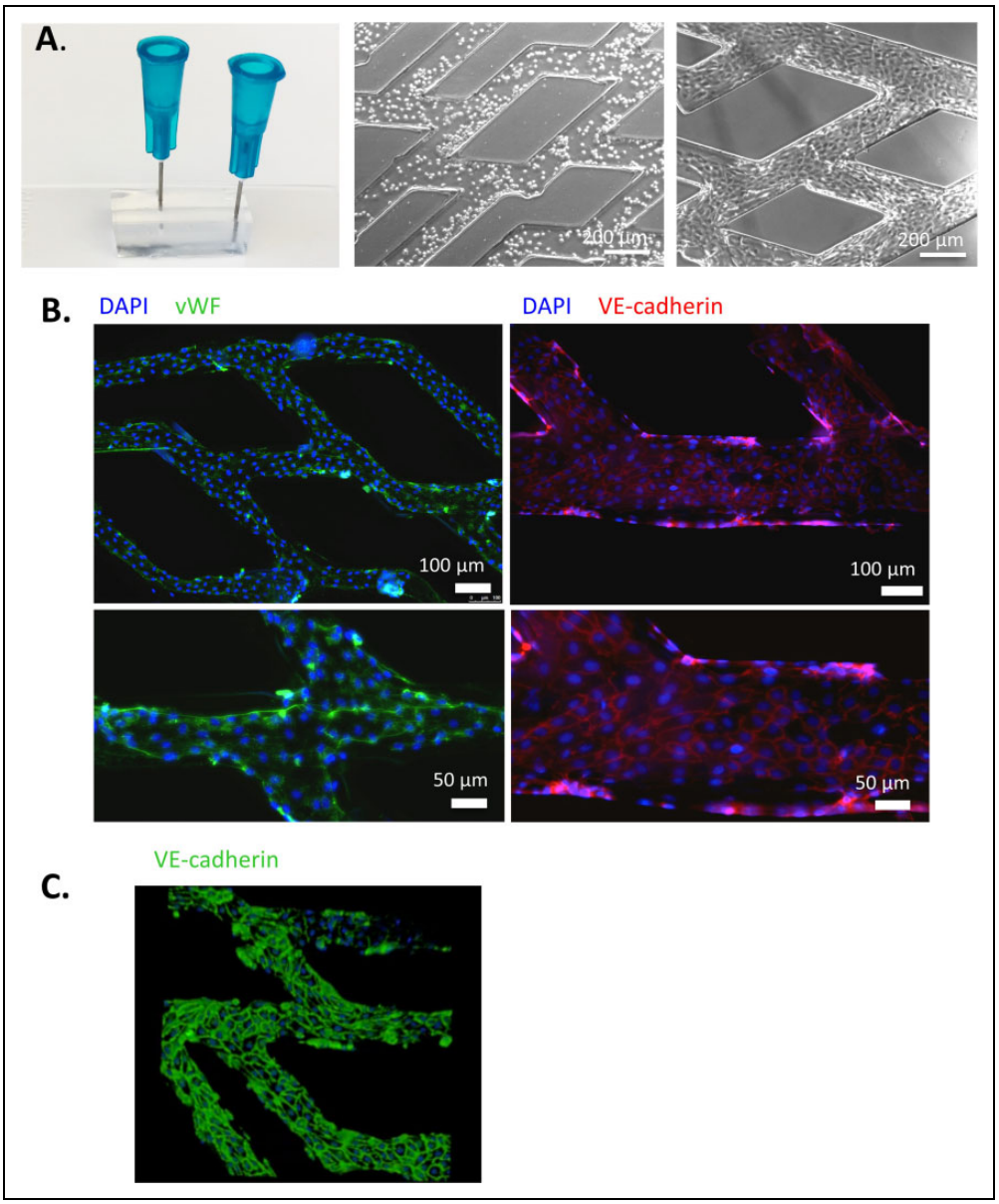

Fig. 5. Physical model of (A) polydimethylsiloxane (PDMS)-microfluidic device attached to glass slide with blunt needles (green) plugged at the inlet and outlet used for seeding of cells and medium replenishment (left), phase-contrast image showing seeding of human umbilical vein endothelial cells (HUVECs; center) and attached and proliferating HUVECs after 4 d of culture in device (right). Immunofluorescence analysis of microvessels generated from HUVECs for (B) von Willebrand factor (vWF; green, top left and bottom left, scale bars = 100 µm and 50 µm, respectively) and vascular endothelial (VE)-cadherin (red, top right and bottom right, scale bars = 100 µm and 50 µm, respectively). (C) 3D confocal micrographs of microvessels generated from hiPSC-ECs showing4, 6-diamidino-2-phenylindole (DAPI) for lumens (blue, left) and VE-cadherin showing intact microvascular junctions (scale bars = 100 µm).

control on bottom), with a level of induction similar to HUVECs, demonstrating that cells are capable of responding to injury. Therefore, hiPSC-ECs appear to be fairly functionally mature cells, with an arterial-like phenotype.

Microvascular Networks in PDMS Microfluidics

HUVECs and hiPSC-ECs were seeded in the PDMS system and cultured for 4 to 7 d. Both cell types attached and proliferated within the channels after initial seeding (Fig. 5A). At the end of the static culture period of 4 to 7 d, immunofluorescence revealed robust coverage by HUVECs, via expression of vWF and VE-cadherin (Fig. 5B). 3D confocal microscopy revealed well-developed junctions as assessed by VE-cadherin (Fig. 5C).

In Silico Modeling of Shear Stress in Microvascular Networks

COMSOL modeling for a 10 µL/min flow condition showed that the velocity (m/s; Fig. 1A) decreased significantly after

encountering the initial bifurcations in the system, while the pressure (Pa) uniformly decreased (Fig. 1B), creating a gradient of pressure through the system with a total pressure drop of 24.1 Pa. The simulated wall shear stress profiles within the device showed a maximum magnitude of 11.3 dyne/cm^2 at the inlet region, which reduced significantly at the middle and outlet regions, and remained highest along the wall and bifurcation points (Fig. 1C). From these calculations, we found that, the operating range of shear stresses was 0.1 to 11.3 dyne/cm^2.

Effect of Flow on Microvessel Phenotype

Literature suggests that shear stress ranges from 19 dyne/cm^2 in arterioles,[24] to 95 dyne/cm^2 in the smallest capillaries of the conjunctiva, to less than 1 dyne/cm^2 in venules.[25] Cultured endothelial progenitor cells increased EphrinB2 expression in a shear stress–dependent manner over the range of 0.1 to 2.5 dyne/cm^2, thus inducing an arterial phenotype.[26,27] This implies that only a small amount of shear stress is necessary to induce phenotypic changes in vascular progenitors. This correlated with our previous study[14] in which shear stress in the range of 5 to 10 dyne/cm^2 was sufficient to have a significant effect on Notch1 signaling in immature hiPSC-ECs. Based upon these observations, we used a maximum shear stress of 11.3 dyne/cm^2, based on COMSOL modeling of the microvascular network, to determine the phenotypic changes imparted by the flow on hiPSC-EC microvessels compared to static controls.

We found that hiPSC-ECs had a random orientation in the static microvessels after 4 to 7 d of culture, whereas after 24 h of continuous laminar flow conditions, they aligned parallel to the direction of the flow (Fig. 6Aand B).[28,29] We also found that shear stress caused changes in the distribution of actin filaments as assessed by immunofluorescence staining for F-actin (Fig. 6 C and D). In static controls, the actin fibers were not elongated (Fig. 6C) but after 24 h of flow, they had long, striated fibers (Fig. 6D).[30] Therefore, in this system, ECs respond to flow in an expected manner.

We found that static microvessels had nonuniform and sparse immunofluorescence for EphrinB2 expression, indicating the lack of an arterial phenotype. However, after 24 h of flow, EphrinB2 expression greatly increased (Fig. 6E and F) with the strongest staining at the edges of the microvessels as well as at the bifurcation points, which corresponded to the high shear regions in the device (Fig. 1C). Therefore, it may be that shear in the range of 0.1 to 11.3 dyne/cm^2 in our system "arterialized" microvessels, with region-specific differences in the expression of EphrinB2.

Lastly, we looked at NO expression. Static microvessels were found to express a low level of NO (Fig. 6G), but shear stress increased the amount of NO secreted (Fig. 6 H) as assessed by immunofluorescence staining using 4-amino-5-methylamino-2',7'-difluroflourescein diacetate. Since NO production has been implicated in vascular remodeling, angiogenesis,[31] and modulating microvascular permeability,[32]

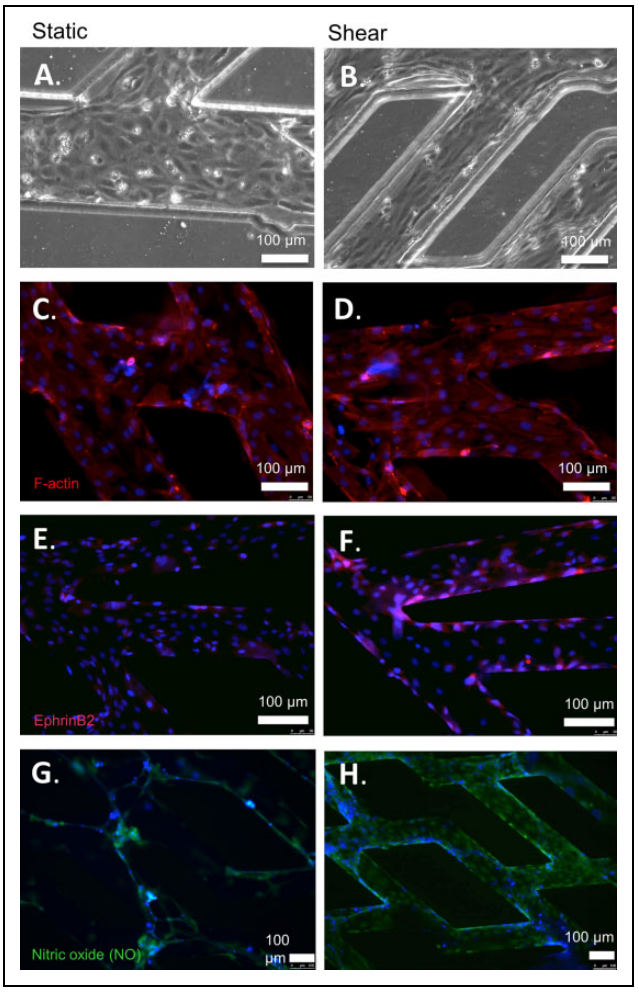

Fig. 6. Phase contrast imaging of (A) static human induced pluripotent stem cell-derived endothelial cell (hiPSC-EC) microvessel morphology compared to (B) morphology of hiPSC-ECs after 24 h of flow. Immunofluorescence analysis of (C) F-actin staining (red) of static hiPSC-ECs compared to (D) F-actin after 24 h of flow. Immunofluorescence staining of (E) EphrinB2 expression (red) in static hiPSC-EC microvessels compared to (F) EphrinB2 expression after 24 h of flow. Live cell immunofluorescence analysis of (G) nitric oxide (NO) production in static hiPSC-EC microvessels compared to (H) NO production after 24 h of flow. Flow condition was 10 µl/mL for 24 h. Scale bars = 100 µm.

these data indicate that the engineered microvessels were behaving in a physiologically relevant manner.

RT-PCR Assessment of hiPSC-EC Microvessel Phenotype

We examined the transcription factors Kruppel-like factor 2 (KLF2/KLF4), venous marker EphB4, and arterial markers Notch1 and EphrinB2 after 24 h of flow as compared to static controls. In assessing venous and arterial marker expression in hiPSC-EC microvessels, we found no significant change in the expression level of the venous marker EphB4, while there were significant increases in both Notch1 and EphrinB2 gene expression (arterial markers) under shear stress (Fig. 7A).

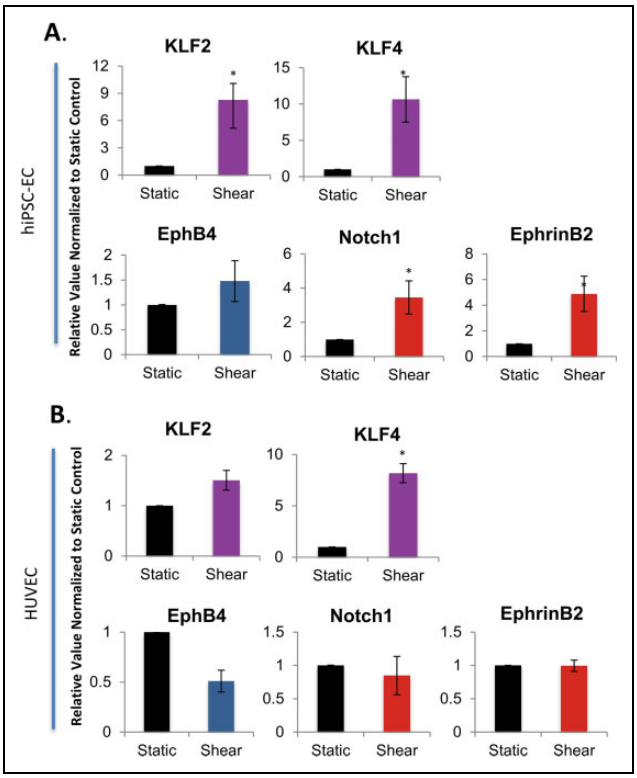

Fig. 7. Quantitative real-time reverse transcription polymerase chain reaction (qRT-PCR) showing gene expression changes under shear compared to static controls for Kruppel-like factor 2 (KLF2), KLF4, Ephrin type-B receptor 4 (EphB4), Notch1 and EphrinB2 in (A) human induced pluripotent stem cell-derived endothelial cell (hiPSC-EC) microvessels and (B) human umbilical vein endothelial cell (HUVEC) microvessels. Values from 3 independent experiments from the triplicate polymerase chain reaction (PCR) reactions for genes of interest were normalized against average glyceraldehyde 3-phosphate dehydrogenase (GAPDH) Ct values from the same complementary DNA (cDNA) sample. Fold change of gene of interest (GOI) transcript levels between samples equals $2\text{-}\Delta\Delta Ct$, where $\Delta Ct = Ct(GOI) - Ct(GAPDH)$, and $\Delta\Delta Ct = \Delta Ct(ATII) - \Delta Ct(ATII)$. Data represented as relative value (shear over static). Asterisks indicate $P < 0.05$. For all panels, data represent at least 3 observations for each experiment and are expressed as mean values $\pm$ standard error of mean.

Interestingly, shear stress did not have any significant impact on EphB4, Notch1, or EphrinB2 gene expression in HUVEC microvessels (Fig. 7B). These data indicate that hiPSC-EC microvessels are more responsive to flow in modulating their phenotype, and possess more plasticity, as compared to HUVECs. We found that shear stress caused an 8.3 and 10.6-fold increase in *KLF2* and *KLF4* gene expression relative to static conditions, respectively, in hiPSC-EC microvessels (Fig. 7A, top). In contrast, in HUVEC microvessels, *KLF2* gene expression was not significantly changed under shear stress, whereas *KLF4* increased 8.2-fold relative to static conditions (Fig. 7B, bottom). Thus, it appears that while HUVECs responded partially to flow, the magnitude and extent of the response are greater in hiPSC-ECs.

Discussion

Microvascular ECs exhibit significant functional heterogeneity in vivo with respect to the organ bed in which they reside.[1] Recent work has demonstrated that human pluripotent stem cells (both hESCs and hiPSCs) can be differentiated into various EC subtypes.[13] Specifically, blood–brain barrier (BBB) ECs were derived from hiPSCs when codifferentiated from neural cells, and the resulting ECs had many BBB attributes, including polarized efflux transporter activity, substantial barrier properties, and well-organized tight junctions.[33] Nevertheless, this protocol required primary cell coculture to derive the brain-specific microvascular ECs, perhaps limiting its potential application. Additionally, Sriram et al. recently described the differentiation of hESCs into almost pure populations of venous and arterial ECs with distinct molecular and functional profiles in vitro through the use of growth factors.[34] These in vitro phenotypic characteristics impacted microvessel structures in vivo, with distinct differences being observed in the Matrigel plug assay, including higher amounts of coverage by perivascular cells in arterial EC-seeded plugs. It needs to be determined whether the enrichment of arterial or venous subtypes provides any therapeutic benefit over a mixed population of ECs.

This study describes the "partial arterialization" of differentiating hiPSC-ECs over the course of 5 d using a 2D, chemically defined and growth factor-free protocol. In addition to significant increases in the gene expression of arterial markers EphrinB2, Notch1, and Connexin 40 on day 5 of differentiation (compared to day 1), Western blot demonstrated sustained protein expression of both NICD and EphrinB2 on all days of differentiation (D1-D5), indicating that this protocol was inducing an arterial-like phenotype from an early time point.

To demonstrate the feasibility of generating intact microvascular networks, we seeded hiPSC-ECs and HUVECs into a PDMS-based microfluidic and exposed them to constant physiological flow. Cells cultured in this manner could upregulate NO and align parallel to the direction of flow, demonstrating flow-sensing ability similar to in vivo microvessels. hiPSC-ECs that were exposed to flow had significantly upregulated EphrinB2 and Notch 1, as well as KLF2 and KLF4, as compared to static controls, indicating an arterial-like, antithrombotic and anti-inflammatory phenotype. However, HUVECs did not have any upregulated arterial markers and demonstrated only a significant increase in KLF4, which indicates that hiPSC-ECs are more plastic in modulating their phenotype under flow than are HUVECs. Since KLF2 appears to be critical in flow-mediated regulation of EC function (while a precise role of KLF4 has yet to be elucidated),[35] these results demonstrate a favorable effect of flow on hiPSC-ECs. These findings could have important implications for the enrichment of ECs toward an arterial-like subtype for microvasular tissue engineering applications.

Some limitations of this study include the use of laminar flow as compared to peristaltic flow, which is more

representative of the in vivo situation, and a single short-term continuous flow condition of 24 h as opposed to a longer term for several days, which could potentially impact the phenotypic changes in the microvessels. Additionally, our model included only ECs, whereas in vivo microvessels are covered by perivascular cells, including smooth muscle cells and pericytes.[36,37] Thus, future improvements should consider coculture models. Lastly, there is a range of shear stress that is present in the device. The global changes seen in the qRT-PCR data could be reflective of small changes throughout, or big changes at the inlet/outlet and little change elsewhere. Since the staining was selected closer to the inlet, further work will require more in depth analysis to correlate the micro-regional physical conditions with the observed changes in phenotype.

The likely mechanism of endothelial specification and induction by CHIR is through the Wnt/β-catenin signaling pathway, in which β-catenin accumulates and travels to the nucleus to activate Wnt target gene expression.[18] Furthermore, evidence reveals a close connection between the Notch signaling pathway, which is involved in regulating arterial marker expression, and canonical Wnt/β-catenin signaling. In fact, dual induction of NICD and β-catenin caused enhanced arterial gene expression during in vivo angiogenesis in adults.[38] Thus, further experimentation to determine whether the convergence of Notch and β-catenin, via a single protein complex of NICD-β-catenin-recombining binding protein suppressor of hairless (RBP-J), can drive arterial fate specification under flow is warranted.

Multiple groups have demonstrated the possible therapeutic benefits of using stem cell–derived ECs for treating diseases, including hind limb ischemia,[39] myocardial infarction,[40] and long-term survival after graft implantation.[41] However, in order to be able to translate such studies into human clinical trials, chemically defined conditions for differentiation that are devoid of xenogeneic components, such as FBS and murine feeder layers, must be developed due to the potential risk of transmission of animal pathogens. hiPSC lines that are reprogrammed using genome integration-free conditions should offer the highest likelihood of success for clinical trials, with the lowest risk profile to patients.

Conclusion

This study demonstrates that PDMS-based microfluidic devices can be used to generate intact microvessels in vitro and can be subjected to shear stress to mimic in vivo physiological conditions. These data show that this system can recapitulate some key biological features of microvessels, including the ability to regulate NO production, cytoskeletal rearrangement, and modulation of phenotype with the application of shear stress. Some important advantages of the hiPSC-ECs used in this report include their phenotypic plasticity, their ability to be derived quickly in a reproducible manner, and their freedom from xenogeneic serum exposure. Since these cells represent a clinically relevant cell source, they are amenable to various applications in regenerative medicine, including drug screening and disease modeling.

Authors' Note

Humacyte produces engineered blood vessels from allogeneic smooth muscle cells for vascular surgery. Humacyte did not fund these studies, and Humacyte did not influence the conduct, description, or interpretation of the findings in this report.

Acknowledgments

The authors would also like to thank Dr Mark Saltzman, Department of Biomedical Engineering, Yale University, for his valuable input for experiments.

Authors' Contribution

LEN designed the research and edited the manuscript; AS differentiated hiPSCs, designed experiments, performed most of the analyses, and wrote the manuscript; MG performed PCR; YX generated microfluidic devices and helped with device setup; EH performed computational modeling of devices; BA performed Western blotting; JZ designed microfluidic devices and provided technical support; CF provided technical input; YQ provided technical input and valuable feedback; and KKH provided technical input and valuable feedback.

Ethical Approval

This study was approved by our institutional review board.

Statement of Human and Animal Rights

This article does not contain any studies with human or animal subjects.

Statement of Informed Consent

There are no human subjects in this article and informed consent is not applicable.

Declaration of Conflicting Interests

The author(s) declared the following potential conflicts of interest with respect to the research, authorship, and/or publication of this article: LEN is a founder and shareholder in Humacyte, Inc., which is a regenerative medicine company. LEN's spouse has equity in Humacyte, and LEN serves on Humacyte's Board of Directors. LEN is an inventor on patents that are licensed to Humacyte and that produce royalties for LEN.

Funding

The author(s) disclosed receipt of the following financial support for the research and/or authorship of this article: LEN has received an unrestricted research gift to support research in her laboratory at Yale. This work was supported by Yale University and by the Connecticut Stem Cell Program grant # 15-RMB-YALE-07 (LEN) and Connecticut Regenerative Medicine Research Fund (RMRF) 12-SCB-YALE-06 (YQ). Support also provided by NIH R01 HL127386 (LEN) and R01 HL116705-01 (YQ).

References

1. Nolan DJ, Ginsberg M, Israely E, Palikuqi B, Poulos MG, James D, Ding BS, Schachterle W, Liu Y, Rosenwaks Z, et al. Molecular signatures of tissue-specific microvascular endothelial cell heterogeneity in organ maintenance and regeneration. Dev Cell. 2013;26(2):204-219.
2. Mendez JJ, Ghaedi M, Sivarapatna A, Dimitrievska S, Shao Z, Osuji CO, Steinbacher DM, Leffell DJ, Niklason LE. Mesenchymal stromal cells form vascular tubes when placed in fibrin sealant and accelerate wound healing in vivo. Biomaterials. 2015;40:61-71.
3. Wells RG. The role of matrix stiffness in regulating cell behavior. Hepatology. 2008;47(4):1394-1400.
4. Lacorre DA, Baekkevold ES, Garrido I, Brandtzaeg P, Haraldsen G, Amalric F, Girard JP. Plasticity of endothelial cells: rapid dedifferentiation of freshly isolated high endothelial venule endothelial cells outside the lymphoid tissue microenvironment. Blood. 2004;103(11):4164-4172.
5. Gimbrone MA, Cotran RS, Folkman J. Human vascular endothelial cells in culture: growth and DNA synthesis. J Cell Biol. 1974;60(3):673-684.
6. Li X, Xu S, He P, Liu Y. In vitro recapitulation of functional microvessels for the study of endothelial shear response, nitric oxide and [Ca2+]i. PLoS ONE. 2015;10(5): e0126797.
7. Zhou J, Niklason LE. Microfluidic artificial "vessels" for dynamic mechanical stimulation of mesenchymal stem cells. Integr Biol (Camb). 2012;4(12):1487-1497.
8. Benam KH, Villenave R, Lucchesi C, Varone A, Hubeau C, Lee HH, Alves SE, Salmon M, Ferrante TC, Weaver JC, et al. Small airway-on-a-chip enables analysis of human lung inflammation and drug responses in vitro. Nat Methods. 2016;13(2):151-157.
9. Whisler JA, Chen MB, Kamm RD. Control of perfusable microvascular network morphology using a multiculture microfluidic system. Tissue Eng Part C Methods. 2013;20(7): 543-552.
10. Shin Y, Han S, Jeon JS, Yamamoto K, Zervantonakis IK, Sudo R, Kamm RD, Chung S. Microfluidic assay for simultaneous culture of multiple cell types on surfaces or within hydrogels. Nat Protoc. 2012;7(7):1247-1259.
11. Qin D, Xia Y, Whitesides GM. Soft lithography for micro- and nanoscale patterning. Nat Protoc. 2010;5(3):491-502.
12. Bhatia SN, Chen CS. Tissue engineering at the micro-scale. Biomed Microdevices 1999;2(2):131-144.
13. Wilson HK, Canfield SG, Shusta EV, Palecek SP. Concise review: tissue-specific microvascular endothelial cells derived from human pluripotent stem cells. Stem Cells. 2014;32(12): 3037-3045.
14. Sivarapatna A, Ghaedi M, Le AV, Mendez JJ, Qyang Y, Niklason LE. Arterial specification of endothelial cells derived from human induced pluripotent stem cells in a biomimetic flow bioreactor. Biomaterials. 2015;53:621-633.
15. Krenning G, Barauna VG, Krieger JE, Harmsen MC, Moonen JR. Endothelial plasticity: shifting phenotypes through force feedback. Stem Cells Int. 2016;2016: e9762959.
16. Adams WJ, Zhang Y, Cloutier J, Kuchimanchi P, Newton G, Sehrawat S, Aird WC, Mayadas TN, Luscinskas FW, García-Cardeña G. Functional vascular endothelium derived from human induced pluripotent stem cells. Stem Cell Reports. 2013;1(2):105-113.
17. Bao X, Lian X, Dunn KK, Shi M, Han T, Qian T, Bhute VJ, Canfield SG, Palecek SP. Chemically-defined albumin-free differentiation of human pluripotent stem cells to endothelial progenitor cells. Stem Cell Res. 2015;15(1):122-129.
18. Lian X, Bao X, Al-Ahmad A, Liu J, Wu Y, Dong W, Dunn Kaitlin K, Shusta Eric V, Palecek Sean P. Efficient differentiation of human pluripotent stem cells to endothelial progenitors via small-molecule activation of WNT signaling. Stem Cell Reports. 2014;3(5):804-816.
19. Takahashi K, Tanabe K, Ohnuki M, Narita M, Ichisaka T, Tomoda K, Yamanaka S. Induction of pluripotent stem cells from adult human fibroblasts by defined factors. Cell. 2007; 131(5):861-872.
20. Yu J, Vodyanik MA, Smuga-Otto K, Antosiewicz-Bourget J, Frane JL, Tian S, Nie J, Jonsdottir GA, Ruotti V, Stewart R, et al. Induced pluripotent stem cell lines derived from human somatic cells. Science. 2007;318(5858):1917-1920.
21. Lee EJ, Niklason LE. A novel flow bioreactor for in vitro microvascularization. Tissue Eng Part C Methods. 2010; 16(5):1191-1200.
22. Haefliger JA, Nicod P, Meda P. Contribution of connexins to the function of the vascular wall. Cardiovasc Res. 2004;62(2): 345-356.
23. dela Paz NG, D'Amore PA. Arterial versus venous endothelial cells. Cell Tissue Res. 2009;335(1):5-16.
24. Stepp DW, Nishikawa Y, Chilian WM. Regulation of shear stress in the canine coronary microcirculation. Circulation. 1999;100(14):1555-1561.
25. Koutsiaris AG, Tachmitzi SV, Batis N, Kotoula MG, Karabatsas CH, Tsironi E, Chatzoulis DZ. Volume flow and wall shear stress quantification in the human conjunctival capillaries and post-capillary venules in vivo. Biorheology. 2007;44(5-6): 375-386.
26. Obi S, Yamamoto K, Shimizu N, Kumagaya S, Masumura T, Sokabe T, Asahara T, Ando J. Fluid shear stress induces arterial differentiation of endothelial progenitor cells. J Appl Physiol. 2009;106(1):203-211.
27. Masumura T, Yamamoto K, Shimizu N, Obi S, Ando J. Shear stress increases expression of the arterial endothelial marker EphrinB2 in murine ES cells via the VEGF-Notch signaling pathways. Arterioscler Thromb Vasc Biol. 2009;29(12): 2125-2131.
28. Baeyens N, Mulligan-Kehoe MJ, Corti F, Simon DD, Ross TD, Rhodes JM, Wang TZ, Mejean CO, Simons M, Humphrey J, et al. Syndecan 4 is required for endothelial alignment in flow and atheroprotective signaling. Proc Natl Acad Sci USA. 2014; 111(48):17308-17313.
29. Akimoto S, Mitsumata M, Sasaguri T, Yoshida Y. Laminar shear stress inhibits vascular endothelial cell proliferation by inducing cyclin-dependent kinase inhibitor p21(Sdi1/Cip1/Waf1). Circ Res. 2000;86(2):185-190.

30. Barbee KA, Davies PF, Lal R. Shear stress-induced reorganization of the surface topography of living endothelial cells imaged by atomic force microscopy. Circ Res. 1994;74(1): 163-171.
31. Kolluru GK, Sinha S, Majumder S, Muley A, Siamwala JH, Gupta R, Chatterjee S. Shear stress promotes nitric oxide production in endothelial cells by sub-cellular delocalization of eNOS: a basis for shear stress mediated angiogenesis. Nitric Oxide. 2010;22(4):304-315.
32. Kubes P, Granger DN. Nitric oxide modulates microvascular permeability. Am J Physiol. 1992;262(2): H611-H615.
33. Lippmann ES, Azarin SM, Kay JE, Nessler RA, Wilson HK, Al-Ahmad A, Palecek SP, Shusta EV. Derivation of blood-brain barrier endothelial cells from human pluripotent stem cells. Nat Biotechnol. 2012;30(8):783-791.
34. Sriram G, Tan JY, Islam I, Rufaihah AJ, Cao T. Efficient differentiation of human embryonic stem cells to arterial and venous endothelial cells under feeder- and serum-free conditions. Stem Cell Res Ther. 2015;6:261.
35. Atkins GB, Jain MK. Role of Krüppel-like transcription factors in endothelial biology. Circ Res. 2007;100(12):1686-1695.
36. Murfee WL, Skalak TC, Peirce SM. Differential arterial/venous expression of NG2 proteoglycan in perivascular cells along microvessels: identifying a venule-specific phenotype. Microcirculation. 2005;12(2):151-160.
37. Hirschi KK, D'Amore PA. Pericytes in the microvasculature. Cardiovasc Res. 1996;32(4):687-698.
38. Yamamizu K, Matsunaga T, Uosaki H, Fukushima H, Katayama S, Hiraoka-Kanie M, Mitani K, Yamashita JK. Convergence of Notch and β-catenin signaling induces arterial fate in vascular progenitors. J Cell Biol. 2010; 189(2):325-338.
39. Lai WH, Ho JCY, Chan YC, Ng JHL, Au KW, Wong LY, Siu CW, Tse HF. Attenuation of hind-limb ischemia in mice with endothelial-like cells derived from different sources of human stem cells. PLoS One. 2013;8(3): e57876.
40. Masumoto H, Ikuno T, Takeda M, Fukushima H, Marui A, Katayama S, Shimizu T, Ikeda T, Okano T, Sakata R, et al. Human iPS cell-engineered cardiac tissue sheets with cardiomyocytes and vascular cells for cardiac regeneration. Sci Rep. 2014;4:6716.
41. Matsuo T, Masumoto H, Tajima S, Ikuno T, Katayama S, Minakata K, Ikeda T, Yamamizu K, Tabata Y, Sakata R, et al. Efficient long-term survival of cell grafts after myocardial infarction with thick viable cardiac tissue entirely from pluripotent stem cells. Sci Rep. 2015;5:16842.